

# Planar Antennas for Far-Field Beam Steering at End-Fire using Directive Surface-Wave Launchers

Symon K. Podilchak<sup>1,2</sup>, Al. P. Freundorfer<sup>2</sup>, Yahia M. M. Antar<sup>1,2</sup>

<sup>1</sup>Royal Military College of Canada, Kingston, ON, Canada

<sup>2</sup>Queen's University, Kingston, ON, Canada

E-mail: antar-y@rmc.ca

**Abstract**—Planar antennas that achieve end-fire radiation by surface-wave (SW) edge diffraction are investigated. Specifically, Yagi-Uda like directive surface-wave launchers (SWLs) are utilized as the surface-wave antenna (SWA) feed, exciting cylindrical SWs on a grounded dielectric slab (GDS). With the design of a recessed ground plane, suitable conditions are achieved for far-field radiation at end-fire. In addition, a novel SWA offering end-fire beam steering is also presented by using a two element array of SWLs. Measured results suggest that the radiated beam pattern can be steered by  $8^\circ$  from  $\phi = -4^\circ$  to  $\phi = +4^\circ$  in the far-field. In addition, highly directive beam patterns are observed from 18.5 - 22.7 GHz suggesting a relatively large radiating bandwidth. To the authors knowledge this is the first time such planar SWAs have been fabricated and measured.

## I. INTRODUCTION

Recently, surface-wave launchers (SWLs) have been utilized as a practical feeding technique for high gain planar leaky-wave antennas (LWAs) at millimeter wave frequencies [1]. In these designs, slotted configurations in the ground plane of a dielectric slab can couple energy into the dominant  $TM_0$  surface-wave (SW) mode exciting bound, cylindrical-waves which propagate along the guiding surface. With the addition of appropriately designed gratings or strips, leaky-waves (LWs) can be excited, realizing the transformation from a bound mode to a radiated mode [2]-[4]. In general, these LWAs are desirable for their low cost and compatibility with other planar devices and monolithic topologies.

Such LWAs offer directive beam scanning as a function of frequency but inherently cannot radiate at end-fire [5]. Thus the use of planar LWAs may be limited for applications where fixed beam patterns over large radiating bandwidths are required. To overcome this limitation simple planar guiding structures, realized by grounded dielectric slabs (GDSs), are presented in this work to achieve directive far-field radiation at end-fire over a significant frequency range. The aforementioned SWLs are utilized as the antenna feed (along with an appropriate GDS) realizing the novel planar surface-wave antennas (SWAs). In addition, single-frequency end-fire beam steering is also presented by using a two element array of SWLs [7] as shown in Fig. 1. To the authors knowledge this is the first time such high gain planar SWAs offering steerable radiation at end-fire have been designed, fabricated and measured for millimeter wave frequencies of operation.

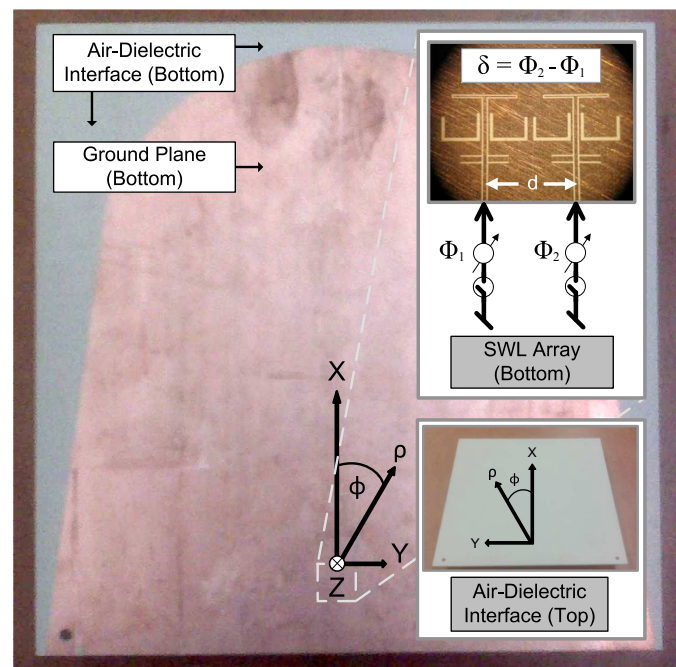


Fig. 1. Realized 2-D planar antenna structure. An array of directive-folded SWLs are used to steer the excited SW field distribution on the guiding surface by changing the relative phase difference between SWL elements ( $\delta = \Phi_2 - \Phi_1$ ) or by turning on/off specific elements. The simple air-dielectric interface defines the guiding structure (top) while the recessed ground plane, conformal to the SWs (bottom), provides suitable conditions for SW edge diffraction realizing end-fire radiation.

## II. DIRECTIVE-FOLDED AND DIRECTIVE-UNFOLDED SURFACE-WAVE LAUNCHERS FOR BOUND PROPAGATION

The planar antenna sources are shown in Fig. 2 and are realized by slots in the ground plane of a GDS ( $\epsilon_r = 10.2$ ,  $h = 1.27$  mm and  $\tan \delta = 0.0023$ ). The main radiating slot of the SWLs excites a cylindrical  $TM$  SW mode and unidirectional SW propagation is achieved by the addition of the secondary reflector slots [1]-[4], [7].

### A. Planar Surface-Wave Launcher Operation

Essentially, the slotted configurations act as magnetic dipole sources for the investigated SWAs. In addition, the SWLs are fed by a coplanar waveguide transmission line, defining a

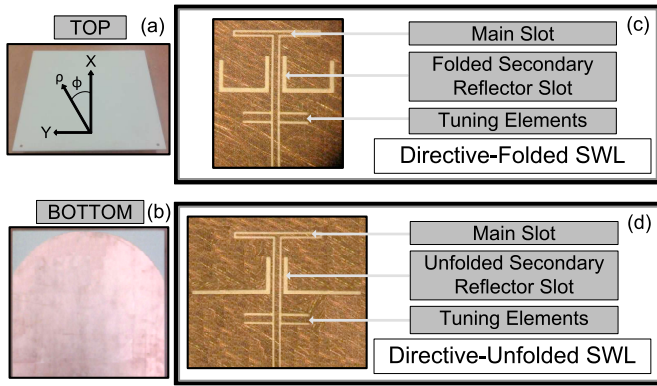


Fig. 2. Investigated planar antenna structures using both folded and unfolded SWL feeds: (a) Air-dielectric interface for guided SW propagation (top). (b) Recessed ground plane and air-dielectric interface conformal to the phase front of the cylindrical SWs (bottom). (c) Directive-folded SWL antenna source. (d) Directive-unfolded SWL antenna source. In these two designs  $r = 0$  mm and  $l = 98$  mm with reference to Fig. 5.

completely planar structure. Two coplanar waveguide shorted stubs match the SW source to the  $50 \Omega$  transmission line feed for measured reflection loss values below 15 dB at 23 GHz as shown in Fig. 3 for both the directive-folded and directive-unfolded SWLs.

### B. Generated Surface-Wave Field Distributions

By the use of a folded [unfolded] secondary reflector slot, the majority of the evanescent SW field distribution (on top of the air-dielectric interface of the GDS) is confined to a  $120^\circ$  [ $150^\circ$ ] 3 dB beam width in the forward  $\hat{x}$  direction as shown in Fig. 4 (a) [(b)]. Essentially, the unfolded secondary slot of directive-unfolded SWL achieves a larger SW beam width when compared to the directive-folded SWL.

To observe such evanescent SW field distributions generated

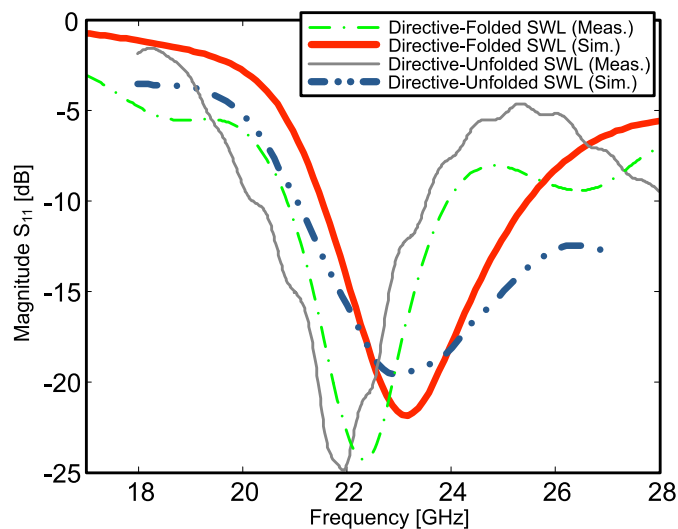


Fig. 3. Reflection loss of the directive-folded and unfolded SWLs. Simulation and measured results are in good agreement. Measured results suggest that the SWLs have reflection loss values greater than 10 dB from 21 to 24 GHz.

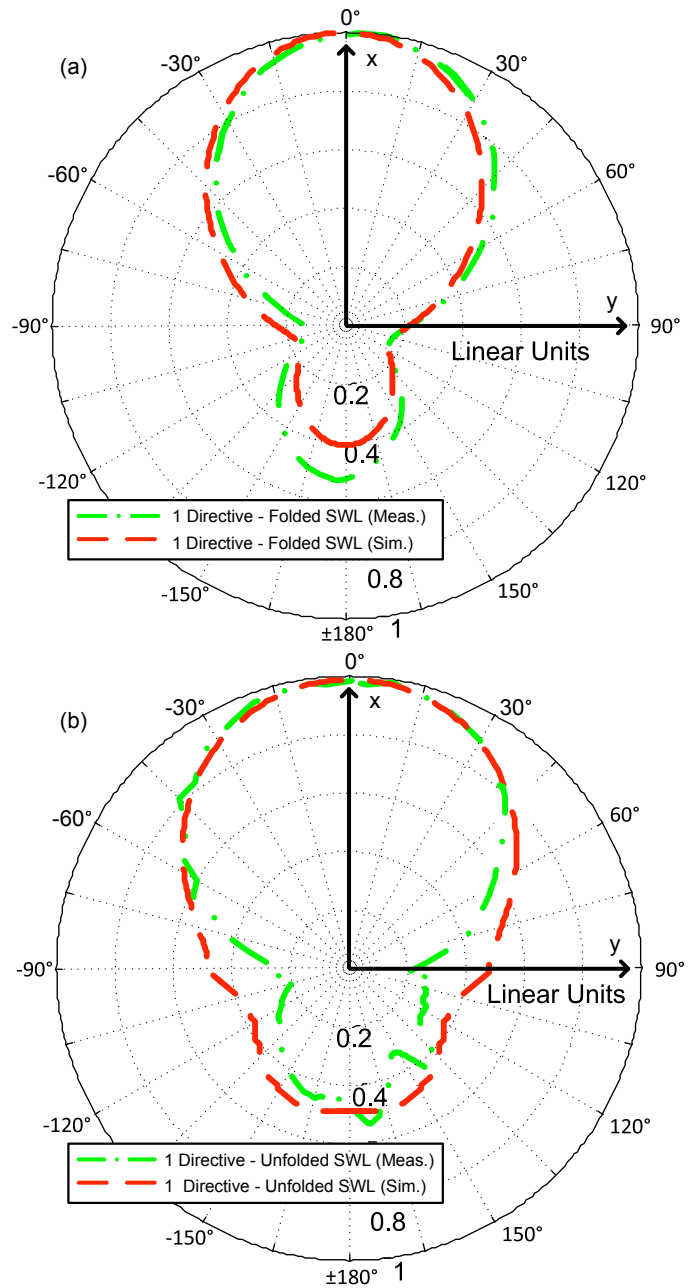


Fig. 4. Measured and simulated SW field distribution for the directive-folded (a) and directive-unfolded (b) SWLs on the guiding surface (normalized and shown in linear units). To measure and simulate the single SW beam patterns, individual SWL elements were placed at the center of a large GDS.

by the SWLs, measurements were completed using a near field probe in  $5^\circ$  steps (on top of the GDS at  $z = 0.5$  mm) on an arc centered (radius,  $r_0 = 4.5$  cm and  $r_0 \gg \lambda^{SW}$ ) at the SWL elements. The measured fields along this arc represent the SW field distributions at a significant distance from the SWL and thus can represent the SW beam pattern on the GDS. In addition, the SWL elements were placed at the center of a large GDS and absorber was used at the edge of slab to minimize unwanted reflections [7]. In addition, simulations

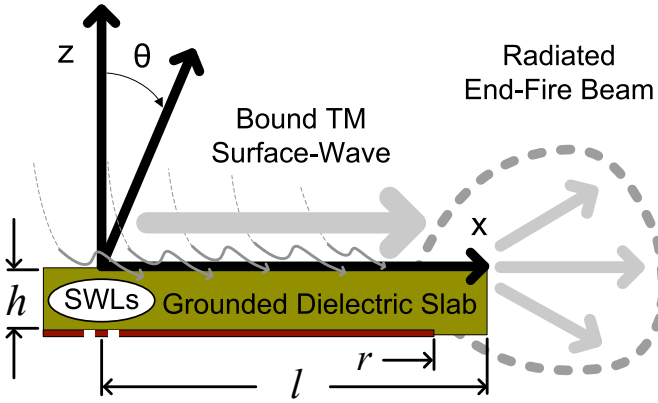


Fig. 5. The SWLs excite a cylindrical  $TM_0$  SW mode on the utilized GDS ( $\epsilon_r = 10.2$ ,  $h = 1.27$  mm,  $\tan \delta = 0.0023$ ,  $l = 93$  mm and  $r = 5$  mm in  $x - y$  plane for Fig. 1, total board size: 15 x 15 cm.). End-fire radiation occurs by edge diffraction on the symmetrical structure.

were completed (assuming an infinite substrate) and results were compared against measured values with good agreement.

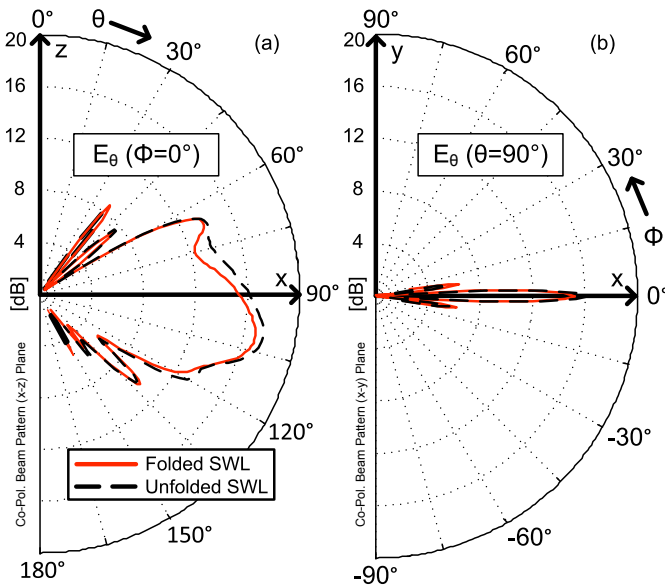


Fig. 6. Radiated end-fire beam patterns from the investigated planar designs using the single folded and unfolded SWL antenna sources. Realized gain results shown in dB for the  $E_\theta$  far-field distribution at 23.8 GHz. (a)  $E_\theta(\phi = 0^\circ)$  in the  $x - z$  plane. (b)  $E_\theta(\theta = 90^\circ)$  in the  $x - y$  plane.

### III. INVESTIGATED PLANAR SURFACE-WAVE ANTENNAS

Three planar surface-wave antennas (SWAs) are presented in this work. Initially, the folded-directive and unfolded-directive SWLs are compared as a single SW source for radiation at end-fire. The investigated structure is shown in Figs. 2 (a) and (b) and the two different directive based SWLs are shown in Fig. 2 (c) and (d). Concepts are then extended

to end-fire beam steering using a two element array of folded-directive SWLs (Fig. 1).

#### A. Theoretical Considerations for Radiation at End-Fire by Surface-Wave Edge Diffraction

By the use of the directive SWLs cylindrical SWs can be generated on the guiding surface as shown in Fig. 5. By the design of a recessed ground plane (total length:  $l$ , and recessed distance,  $r$ ), SWs can radiate by edge diffraction at the end of the guiding structure [5], [6] and the far field beam pattern,  $P(\theta)$ , in the  $x - z$  plane can be approximated by

$$P(\theta) = \frac{\sin\left(\frac{l}{2}(\beta^{SW} - k_0 \sin \theta)\right)}{\frac{l}{2}(\beta^{SW} - k_0 \sin \theta)}, \quad (1)$$

where,  $\beta^{SW}$  is the SW propagation constant along the radial direction and  $k_0$  defines the free space wavenumber. Gain values from 12 dB to 20 dB can be observed for such SWAs using a single source [5].

Physically, the large ground plane provides a significant [minimal] antenna aperture for edge diffraction in the  $x - y$  [ $x - z$ ] plane and thus narrow [broad] beam widths can be observed in the far-field. In addition, the recessed ground plane at the end of the slab increases the effective aperture of the SWA in the  $x - z$  plane. For instance, the evanescent SW field distribution is spread out as the propagating SWs approach the edge of the board; ie. evanescent SWs are free to propagate in the upper and lower  $\pm z$  free space regions for  $l - r \leq x \leq l$ . Furthermore, the abrupt change in boundary conditions perturbs the propagation constant ( $\beta^{SW}$ ) of the traveling SW along the guiding surface causing a lensing effect. In addition, circular ground plane designs are optimal to be conformal to the cylindrical SW phase front generated by the directive SWLs.

#### B. Investigated Surface-Wave Antennas Using a Single Source

Results for the two SWAs (Fig. 2) using the folded-directive and unfolded-directive single SWL sources are shown in Fig. 6 at 23.8 GHz. As expected broad [narrow] beam patterns are observed in the  $x - z$  [ $x - y$ ] plane due to the relatively minimal [large] antenna aperture. In these designs the recessed ground plane distance (in the  $x - z$  plane) is set to zero ( $r = 0$ ) and simulated gain values are above 15 dB. As expected, the SWA using the unfolded-directive SWL, achieved higher gain values (when compared to the folded-directive SWA) by  $\approx 1$  dB due to the increased beam width generated by the unfolded SWL, as shown in the SW field distribution of Fig. 4 (b).

#### C. Beam Steering at End-Fire Using a Two Element Array of Folded-Directive Surface-Wave Launchers

End-fire beam steering is shown using the two element array of folded-directive SWLs [7]. Results for the fabricated structure of Fig. 1 are shown in Fig. 7 for varied relative phase difference between SWLs elements ( $\delta = 0^\circ, -30^\circ, -60^\circ$  and  $+90^\circ$ ). Simulated gain values are above 14 dB at 22.6 GHz. In addition, increased beam steering is possible by turning on and off the SWL elements [7].



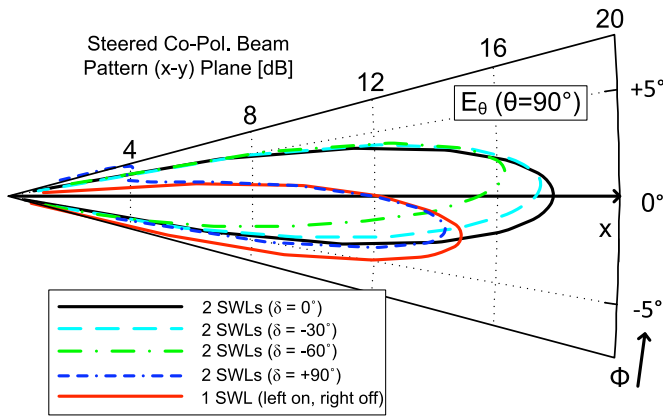


Fig. 7. Steered beam pattern at end-fire using the two element array of directive-folded SWLs and the antenna structure of Fig. 1. Realized gain in dB for the  $E_\theta(\theta = 90^\circ)$  far-field distribution in the  $x - y$  plane. By varying the relative phase difference and by adjusting the effective weighting between SWLs (by turning on and off elements) the main beam can be steered within  $\phi \in [-4^\circ, +4^\circ]$  while maintaining gain values above 14 dB at 22.6 GHz.

Measured 2-D beam patterns are shown in Fig. 8 over a broad frequency range from 18.5 GHz to 22.7 GHz for  $\delta = 0^\circ$ . Furthermore, Fig. 9 illustrates the observed beam steering at end-fire by turning on and off the left and right SWL elements; ie. the far-field beam pattern can be steered by  $8^\circ$  from  $\phi = \pm 4^\circ$  at 21 GHz in the  $x - y$  plane.

#### IV. CONCLUSION

This work has presented directive-folded and directive-unfolded surface-wave launchers (SWLs) for end-fire radiation by surface-wave (SW) edge diffraction. Far-field beam patterns with gain values above 15 dB are shown for the two designs using such single SWL elements. In addition, by using a two element of array of directive-folded SWLs, measured beam scanning at end-fire is observed. Results suggest that the main radiated far-field beam can be steered by  $8^\circ$  at end-fire with gain values greater than 14 dB.

#### REFERENCES

- [1] S. Mahmoud, Y.M.M. Antar, H. Hammad, and A. Freundorfer, "Theoretical considerations in the optimization of surface waves on a planar structure," *IEEE Trans. Antennas Propag.*, vol. 52, no. 8, pp. 2057–2063, Aug. 2004.
- [2] M. Ettorre, S. Bruni, G. Gerini, A. Neto, N. Llombart, and S. Maci, "Sector PCS-EBG Antenna for Low-Cost High-Directivity Applications," *IEEE Antennas and Wireless Propagation Lett.*, vol. 6, pp. 537–539, 2007.
- [3] S.K. Podilchak, A.P. Freundorfer and Y.M.M. Antar, "Planar Leaky-Wave Antenna Designs Offering Conical-Sector Beam Scanning and Broadside Radiation using Surface-Wave Launchers," *IEEE Antennas and Wireless Propagation Lett.*, vol. 7, pp. 155–158, 2008.
- [4] S.K. Podilchak, A.P. Freundorfer and Y.M.M. Antar, "New Planar Antenna Designs Using Surface-Wave Launchers for Controlled Leaky-Wave Beam Steering," APS-URSI 2008, San Diego, California, USA., Jul. 2008.
- [5] F. J. Zucker, "Surface-Wave Antennas, in *Antenna Theory, Part 2*. R. E. Collin and F. J. Zucker." New York, USA: McGraw-Hill, 1969.
- [6] C. H. Walter, "Traveling Wave Antennas" New York, USA: McGraw-Hill, 1965.
- [7] S.K. Podilchak, A.P. Freundorfer and Y.M.M. Antar, "Surface-Wave Launchers for Beam Steering and Application to Planar Leaky-Wave Antennas," *IEEE Trans. Ant. Prop.*, Accepted Oct. 2008.

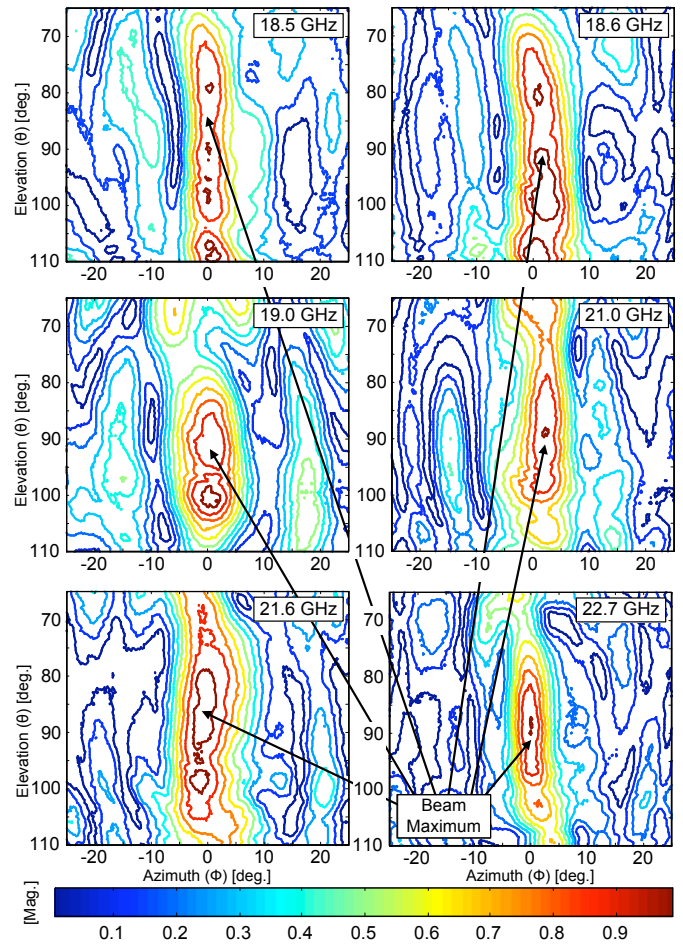


Fig. 8. Measured end-fire gain patterns,  $E_\theta$ , in linear units and normalized to observed maximum. Results shown for  $f = 18.5, 18.6, 19.0, 21.0, 21.6$  and  $22.7$  GHz.

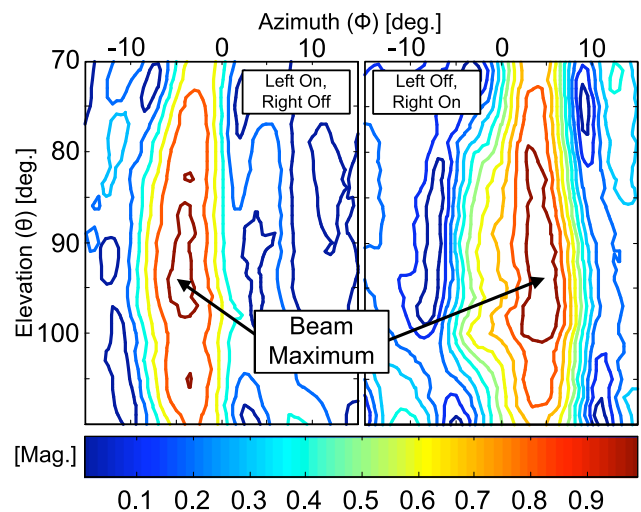


Fig. 9. Measured end-fire gain patterns,  $E_\theta$ , in linear units and normalized to observed maximum at 21 GHz. By turning on and off the left and right SWL elements beam steering can be achieved at end-fire from  $\phi = \pm 4^\circ$ .